Investigating the orientation dependence of non-linear GRE phase evolution in White Matter using a high resolution geometric magnetic susceptibility WM model

Way Cherng Chen[1,2], Sean Foxley[1], and Karla Miller[1]

[1]*FMRIB Centre, University of Oxford, Oxford, Oxon, United Kingdom,* [2]*Magnetic Resonance Imaging Group, Singapore Bioimaging Consortium, Singapore, Singapore, Singapore*

Introduction Susceptibility-weighted contrast in white matter is a topic of recent interest due in part to intriguing observations of signal dependence on tract orientation to B0. Non-linear GRE phase evolution has been previously reported (1,2) and the source has been proposed to be related to the underlying white matter (WM) tissue microstructure. In this study, we investigated the orientation dependence of non-linear GRE phase evolution in WM and compared the results with simulations from a realistic geometric model of WM microstructure (3), including the potential contribution of intrinsic susceptibility anisotropy (7).

Methods *MRI protocol.* In-vivo experiments on seven healthy volunteers were conducted on a 3.0T Siemens Trio MRI scanner with a 12-channel head coil. A 2D multi-echo GRE sequence was used to obtain phase images (TE=4-60ms, ΔTE=8ms ,TR=1.5s, 2×2×2mm, 10 averages). Unwrapping of the signal phase was performed on a voxel-by-voxel basis in 1D across echoes. DTI data (2×2×2mm, b=1000 s/mm^2, 30 directions) was used to determine the orientation of WM fibers relative to B_0. WM voxels were divided into 6 groups according to their principle alignment with B_0 (θ=0-15°,15-30°,30-45°,60-75°,75-90°). The mean phase evolution of grey matter (GM) voxels was subtracted from WM voxel phase time series. Deviation from linear phase evolution was calculated for each voxel by subtracting the best-fit line from the phase time series to give the "phase residue". *Model description.* The geometric model consists of a circular bundle of WM fibers surrounded by a reference medium. The WM fiber bundle is divided into 3 micro-compartments: axon, myelin and extra-axonal space. Each axon is modelled as an infinite cylinder with myelin represented as an annular ring surrounding the axon with a pre-defined g-ratio of 0.65. Axons are densely-packed at random locations with axon diameter following a gamma distribution to yield a volume fraction of 0.7. Magnetic susceptibility and T2 values for the compartments are taken from literature (χ_{my}=-0.08ppm (4), $\chi_{ax}=\chi_{ea}$=0ppm, T_{2my}=25ms, $T_{2ea}=T_{2ea}$=75ms (5)), and the proton density of myelin is taken to be half that of the other compartments.. The axonal bundle is simulated over a range of orientations with respect to B_0. The magnetic field on the simulated grid was calculated using analytical solutions for infinite cylinders (6). Magnetization evolution at each grid point is calculated using Bloch equations with short time steps, and the signal is calculated as the complex sum over the WM fiber bundle. Diffusion and water exchange across compartments are assumed to be negligible. A simulation with bulk susceptibility anisotropy of the myelin compartment was performed, where $\chi(\theta) = \chi_{\parallel} + \chi_{aniso}\sin^2(\theta)$ (7) and $\chi(90°)$ = -0.08ppm and χ_{aniso}= - 0.04ppm (8).

Results. The experimental phase evolution curves revealed significant deviations from linearity (Fig 2a), as reported previously (1,2). More interestingly, WM voxels at different orientation to B_0 show different trends of deviation from linear phase evolution. The phase residue for perpendicular fibers (75°<θ<90°) shows an approximately positive quadratic trend while that of parallel fibers (0°<θ<15°) shows an approximately negative quadratic trend. The geometric model predicts similar trends with echo time (Fig 2b). In this model, deviation from linear phase evolution is caused in part by compartmentalization of magnetic susceptibility. This leads to an asymmetric frequency distribution (as can be seen in Fig 1c) such that signal from positive and negative frequency offsets do not cancel equally at all time points. Differences in T_2 between frequency-shifted compartments can also bring about a non-linear phase evolution; however, the observed orientation dependence must be caused by susceptibility effects since T_2 is orientation independent. This phenomenon illustrates an important difference between our model and the simpler approach of approximating the distribution from the field generated outside a single cylinder characterized by a mean magnetic susceptibility: the latter model always predicts a linear phase evolution, while ours encapsulates non-linear evolution. Introducing susceptibility anisotropy actually reduces the amplitude of the phase residues, which is arguably in better agreement with experimental results (Fig 2c). However, bulk magnetic anisotropy *does not* generate the non-linear phase evolution.

Discussion and Conclusions. Wharton (2) has previously introduced a similar hollow-cylinder model by looking at the field perturbation caused by a representative single white matter fiber incorporating isotropic and anisotropic magnetic susceptibility and chemical exchange. By fitting compartmental T_2, g-ratio, exchange rates etc, that work reproduced experimentally-observed non-linear phase evolution trends in WM. A major difference in our model is that we explicitly model the microstructural arrangement of the densely-packed WM fibers (e.g packing, distribution, diameters, etc). Single cylinder approximations have been successfully used to model networks such as blood vessels in the brain to study BOLD contrast characterized by low volume fraction. The high volume fraction of the WM fibers leads to interactions of the magnetic fields generated by individual fibers. Thus, some signal properties may not be well modelled by a single fibre. Finally, it is important to stress that ours is an entirely forward model: no parameters were fit, but rather were based on literature. We have previously shown that this forward geometric model can be used to account for the orientation modulation of mean GRE phase and T2* and also predict the observed deviation from mono-exponential T2* decay (3). These results are summarized in Fig 3 to emphasize that a forward model using a consistent set of parameters taken from the literature is able to predict a broad range of observed signal phase and magnitude properties. Here we have further shown that the same model also predicts higher order signal characteristics such as the non-linear phase evolution. An important implication from our geometric model is that susceptibility compartmentalization is the driving force behind the various GRE signal characteristics and susceptibility anisotropy modulates but does not drive the signal characteristics.

References. (1) Schweser ISMRM 2011. (2) Wharton PNAS 2012. (3) Chen ISMRM 2012. (4) Liu NeuroImage 2011. (5) Laule J Neurol 2004. (6) Haacke Wiley 1999. (7) Lee PNAS 2010. (8) Boroske Biophy. Journ. 1978.

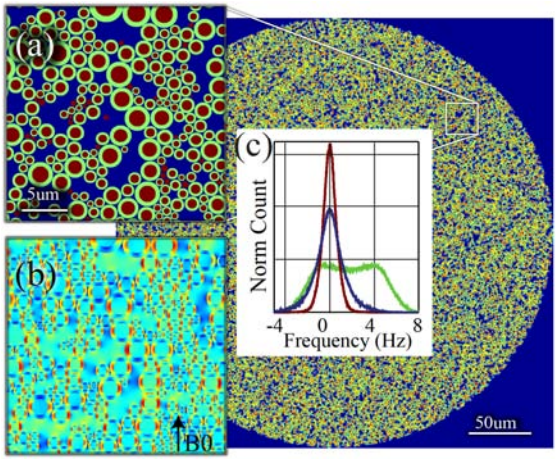

Figure 1: 2D geometric model of white matter (WM). (a) Approximately 50000 WM fibers were modelled in a circular bundle with a close random packing. White box shows a zoomed in illustration of the WM microstructure. Dark blue=extra-axonal space, green=myelin, red=axon. (b) The frequency map generated in presence of an external magnetic field B0. (c) Corresponding frequency histogram for each compartment.

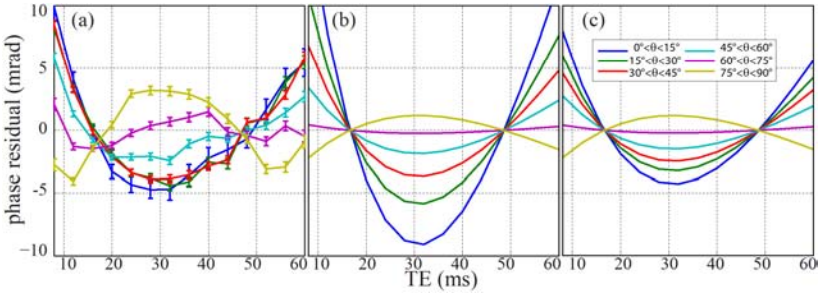

Figure 2. Non-linear phase evolution dependence on orientation. Fig 1a shows the experimental results of the phase residual from WM voxels with different orientations to B0. Error bar indicates standard error across subjects. Fig 1b shows simulation results from our geometric WM model without magnetic susceptibility anisotropy in myelin. Fig 1c shows simulation results with magnetic susceptibility anisotropy in the myelin compartment.

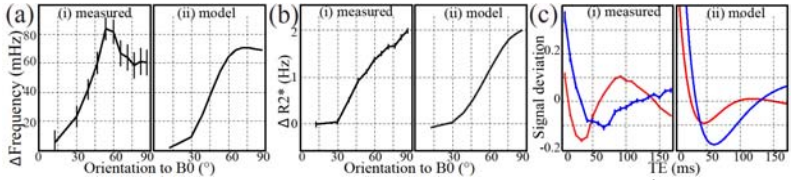

Figure 3: Frequency and R2* modulation with orientation to B0. (a) Measured and simulated frequency modulation. (b) Experimental and simulated R2* modulation. (c) Experimental and simulated deviation from mono-exponential decay (signal magnitude minus R2* decay fit). Error bars indicate the standard error across all subjects.